PHYSICAL REVIEW C VOLUME 49, NUMBER 3 MARCH 1994

Quasielastic scattering of ^{12,14}Be on ^{12}C

M. Zahar, M. Belbot, J. J. Kolata, K. Lamkin, and R. Thompson
Physics Department, University of Notre Dame, Notre Dame, Indiana 46556

J. H. Kelley, R. A. Kryger, D. J. Morrissey, N. A. Orr,* B. M. Sherrill, J. S. Winfield, and J. A. Winger†
National Superconducting Cyclotron Laboratory, Michigan State University, East Lansing, Michigan 48824

A. H. Wuosmaa
Physics Division, Argonne National Laboratory, Argonne, Illinois 60439
(Received 18 November 1993)

The quasielastic scattering of the exotic neutron-drip-line nucleus ^{14}Be on a ^{12}C target has been studied at an incident energy of 796 MeV, and compared with that of the ^{12}Be "core" at the same energy per nucleon. Evidence is presented that the phenomenological optical-model potential for the former system requires an attractive real surface term, as well as the "expected" surface imaginary term, in order to reproduce the experimental angular distribution.

PACS number(s): 25.70.Bc, 24.10.Ht, 27.20.+n, 25.60.+v

The exotic nature of very neutron-rich light nuclei such as ^{6,8}He, ^{11}Li, and ^{11,14}Be has by now been well established. Reviews of the most important experiments, essentially all of which address either ^{11}Be or ^{11}Li nuclei, are given in Refs. [1] and [2]. On the other hand, the ^{14}Be system might be of even more interest than ^{11}Li since the wave function of the last two neutrons in ^{14}Be is expected to contain a larger $(2s_{1/2})^2$ shell-model component. In this configuration, the "tail" of the wave function should extend to large distances as it does not encounter an angular momentum barrier. In addition, the two-neutron separation energy of ^{14}Be is much larger than that of ^{11}Li, and it could prove very interesting to study the effect of that extra binding on the structure and reactions of this nucleus. Previous works [3–5] on the elastic scattering of "halo" nuclei has shown that the experimental angular distributions tend to be considerably different from those measured for nearby, more stable (but still radioactive) nuclear beams. However, except in the case of the proton-scattering experiment of Moon *et al.* [4], the theoretical analysis has been hampered by the lack of direct comparison to the scattering of the "core" of the halo system, which would make the extraction of the effect of the neutron halo more feasible. In general, existing calculations using Glauber-model folding potentials (see, e.g., the discussion in Ref. [6]) predict enhanced absorption due to the presence of the "halo" neutrons, but also a reduction in the strength of the real potential, while a phenomenological optical-model analysis [7] seems to require enhancements in both the real and imaginary parts of the potential.

In the present experiment, we have studied the quasielastic scattering of ^{12,14}Be on ^{12}C at an incident energy of 56 MeV/nucleon. The secondary beams were produced by fragmentation of an 80 MeV/nucleon ^{18}O beam on a 790 mg/cm ^{2}Be target, and separated using the A1200 Fragment Separator at Michigan State University. The purity of the beams was enhanced by the use of a 515 mg/cm^2 plastic achromatic wedge. All remaining beam impurities were identified by time-of-flight techniques. The energy width of the beam, defined by the momentum acceptance of the A1200 spectrometer, was 6%. The beam intensity was adjusted to $< 10^4$ particles per second (pps) for ^{12}Be, while the on-target rate of ^{14}Be varied from 100–200 pps during the course of the experiment. The elastic scattering angular distributions on a $^{\rm nat}$C target were measured after transporting the secondary beam to a scattering chamber. The transverse acceptance of the A1200 spectrometer and beam transport lines is approximately 40π mm mrad, leading to a beamspot that is typically 9 mm in diameter, with a divergence of about 0.8° full width at half maximum (FWHM). In order to achieve the required angular resolution, we used a system that reconstructed the angle and position of each incident particle as it struck the target. A schematic view of the experimental setup is given in Fig. 1. The incident particles were tracked onto the target using two x-y position-sensitive parallel-plate avalanche counters (PPACs) separated by 1 m; their position resolution of 2 mm in the vertical and horizontal planes led to an angular uncertainty of 0.15° FWHM in the direction of the beam. The scattered particles were detected in one of three Si-CsI telescopes which spanned the angular range from 0° to 10° in the laboratory frame (the zero-degree telescope also monitored the composition and intensity of the ^{12,14}Be beam). All of the telescopes consisted of a 300 μm thick by 5 cm square Si ΔE detector, a 300 μm thick by 5 cm square double-sided (x-y) strip detector having 16 strips in each direction, and a CsI stopping detector with photodiode readout. The corresponding angular resolution was 0.19° in the forward

*Present address: LPC-ISMRA, Boulevard du Marechal Juin, 14050 Caen Cedex, France.

†Present address: Cyclotron Institute, Texas A&M University, College Station, TX 77843-3366.

 ©1994 The American Physical Society

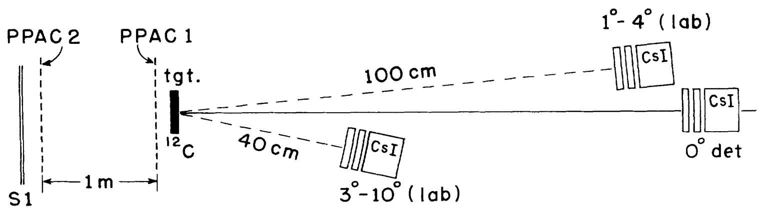

FIG. 1. Schematic diagram of the experimental setup.

telescopes and 0.44° in the backward telescope; multiple scattering in the 250 mg/cm^2 thick secondary target gave an additional contribution of 0.3° FWHM. Thin scintillators placed just upstream of the first PPAC (see Fig. 1) and immediately following the A1200 (separation of 30 m) allowed us to measure the incident-particle energy to about 1.35% FWHM via time of flight. The mean beam energy at the center of the target was 56.7 ± 0.1 MeV per nucleon, for both ^{14}Be and ^{12}Be projectiles. The experimental apparatus differs in two important ways from that used in our previous experiment [3]. First of all, the additional ΔE detectors in each telescope gave redundant identification of the scattered particle. Secondly, the time-of-flight information allowed for a more complete separation of beam impurities and much improved energy resolution, which restricts the contribution from inelastic scattering to high-lying states in ^{12}C, though we were still unable to resolve the low-lying 2^+ and 3^- states.

The angular distribution obtained from the ^{12}Be quasielastic group is shown in Fig. 2, as a ratio to the Rutherford cross section. A cutoff at small angles was imposed to ensure that only particles interacting in the target are included in these data. The minimum required defection of 1° (3σ for the angular resolution) eliminates, for example, all events in which the ^{12}Be reacts in the zero-degree detector rather than in the target. The error bars include an estimate of the effect of the angular resolution of the detectors on the measured cross section, which is particularly significant at small angles where the yield is rapidly changing.

The solid curve in Fig. 2 is the "best-fit" result of a phenomenological optical-model analysis similar to that performed by Mermaz [7] for our earlier ^{11}C and ^{11}Li data [3]. We also used the automatic search code ECIS88 of Raynal [8], and accounted for inelastic scattering to the 2^+ and 3^- states in ^{12}C by adding the predicted cross section for these states to the ground-state (g.s.) elastic yield, and averaging over the angular resolution of the detector system before comparison with experiment. One difference between this analysis and that of Mermaz is that the angular distribution for the 2^+ state has been calculated in the coupled-channels approach rather than in the distorted-wave Born approximation (DWBA), since the coupling between this state and the g.s. is strong. The form factor for this transition was computed in the rotational model, deforming both the real and imaginary wells with deformation parameter β_2=0.592 [9]. The angular distribution of the 3^- state was calculated using the DWBA approach in the vibrational model, with β_3=0.40 [10]. The individual components of the calculation given in Fig. 2 are illustrated separately in Fig. 3.

The fit shown in Fig. 2 has $\chi^2/N = 1.0$, where N is the number of data points; the optical-model parameters corresponding to this fit are given in Table I. This is a volume Woods-Saxon potential, with a small surface imaginary part (normalized derivative of a Woods-Saxon shape) added to improve the fit in the center-of-mass (cm) angular range near 6°. Except for the much deeper

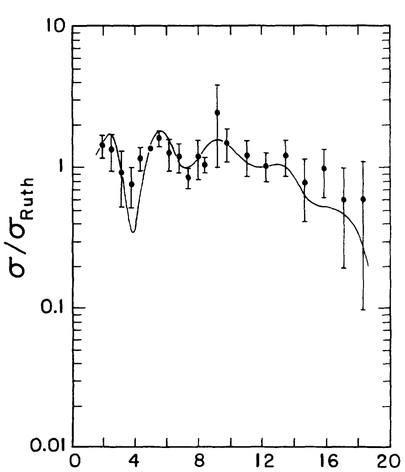

FIG. 2. Quasielastic-scattering angular distribution for ^{12}Be on ^{12}C at an incident energy of 679 MeV. The solid curve is the result of the phenomenological optical-model calculation discussed in the text.

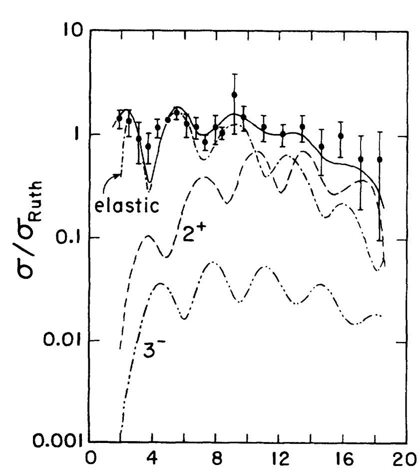

FIG. 3. As in Fig. 2, except that the dotted curve shows the prediction for pure elastic scattering, while the dashed and dot-dash curves are the calculation for inelastic scattering to the 2^+ and 3^- states of ^{12}C, respectively.

TABLE I. Optical-model parameters for various projectiles on a ^{12}C target. The Coulomb radius is equal to the radius of the real-volume term, r_0. The A=11 potential are from Ref. [7].

Projectile	^{11}C	^{12}Be	^{14}Be	^{11}Li
E_{lab} (MeV)	620.0	679.0	796.0	637.0
V (MeV)	40.0	40.0	40.0	40.0
r_0 (fm)	0.990	0.990	0.838	1.015
a_0 (fm)	0.981	0.932	0.694	1.055
W (MeV)	25.92	74.76	86.75	20.73
r_i (fm)	0.986	1.003	1.003	1.077
a_i (fm)	0.407	0.497	0.716	0.457
V_s (MeV)			2.916	2.26
r_{0s} (fm)			1.954	1.950
a_{0s} (fm)			0.556	1.201
W_s (MeV)		0.359	2.319	1.18
r_{is} (fm)		1.753	1.806	1.646
a_{is} (fm)		0.213	0.249	0.544
σ_{reac} (mb)	801.0	1238.0	1900.0	1248.0
σ_{2^+} (mb)	36.6	26.2	30.0	36.7
σ_{3^-} (mb)	13.0	4.0	10.3	13.2
χ^2/N	2.4	1.0	2.1	2.0

imaginary well and the surface-imaginary term, this potential is qualitatively very similar to that given by Mermaz [7] for our ^{11}C data, also shown in Table I. In fact, we found that the already good fit to the ^{11}C data obtained by Mermaz can be improved by the addition of a small surface-imaginary potential as in the current analysis.

Because of the much deeper imaginary well, the reaction cross section deduced from the ^{12}Be potential given in Table I (σ_r=1238 mb) is very much greater than that calculated for ^{11}C (σ_r = 800 mb), and it is important to discuss whether this is a reasonable result. In this discussion, we follow the parameterization of the total reaction cross section given by Kox et al. [11]:

$$\sigma_{\mathrm{reac}}(\mathrm{mb}) = 10\pi R^2(1 - B/E_{\mathrm{cm}}), \quad (1)$$

where

$$R = r_{0t}A_t{}^{1/3} + r_{0p}A_p{}^{1/3} + \mu(1.85 + \beta' E_{\mathrm{cm}}{}^{-1/3}) - C(E) + \alpha(Z_t/A_t)[(A_p - 2Z_p)/A_p].$$

In this formula

$$\mu = (r_{0t}A_t{}^{1/3} r_{0p}A_p{}^{1/3})/(r_{0t}A_t{}^{1/3} + r_{0p}A_p{}^{1/3})$$

with $r_{0i} = 1.1$ fm,

where $i = p, t$ for the projectile and target, respectively. The two energy-dependent factors are $\beta' = 0.160$ MeV$^{1/3}$ and $C(E) = 1.365$ fm at a laboratory energy of 56 MeV per nucleon. The neutron-excess term, with coefficient $\alpha = 5$ fm, has been rewritten to take account of the fact that the projectile rather than the target has nonzero isospin in our experiment. Finally, B is the height of the Coulomb barrier which we compute using the procedure followed by Shen Wen-qing et al. [12] in their analysis of reaction cross section data:

$$B = 1.44(Z_tZ_p)/r - b(R_tR_p)/(R_r + R_p), \quad (2)$$

where $b = 1$ MeVfm^{-1} and

$$r = R_t + R_p + 3.2 \text{ fm},$$

$$R_i = 1.12A_i{}^{1/3} - 0.94A_i^{-1/3} \ (i = p, t).$$

Using this formula and *neglecting the isospin-dependent term for the moment*, we find a total reaction cross section for ^{12}Be+^{12}C of 1130 mb, slightly smaller than the value of 1238 mb obtained from the coupled-channels analysis. Tanihata et al. [13] have shown, however, that the ^{12}Be radius calculated using Eq. (1) above is slightly smaller than that required by their experimental reaction cross section data taken at about 800 MeV per nucleon incident energy. Substituting their larger value of 2.57 fm, we find σ_{reac}=1160 mb for the present case, in better agreement with experiment and well within the estimated 10% uncertainty of the parametrization [11]. On the other hand, if we now include the neutron-excess term, the computed cross section increases to 1495 mb, i.e., 20% larger than our measured value. This might be construed as evidence that the parameter α, determined from elastic scattering on a series of Ni isotopes, is too large to account for the experimental results in this lighter-mass regime, or that the dependence on the neutron excess is not linear. Note, however, that the total reaction cross section obtained by Mermaz for ^{11}C+^{12}C (800 mb) is also somewhat smaller than the value of 1020 mb calculated for this system using the procedure given above. In any event, it is clear that the experimental total reaction cross section of 1238 mb is not unreasonably large.

The angular distribution measured for quasielastic scattering of ^{14}Be on ^{12}C is shown in Fig. 4. In comparison with the ^{12}Be+^{12}C data (Fig. 2), it can be seen that the ratio-to-Rutherford value is typically suppressed by somewhat less than a factor of two, as might be expected due to the extra absorption induced by the

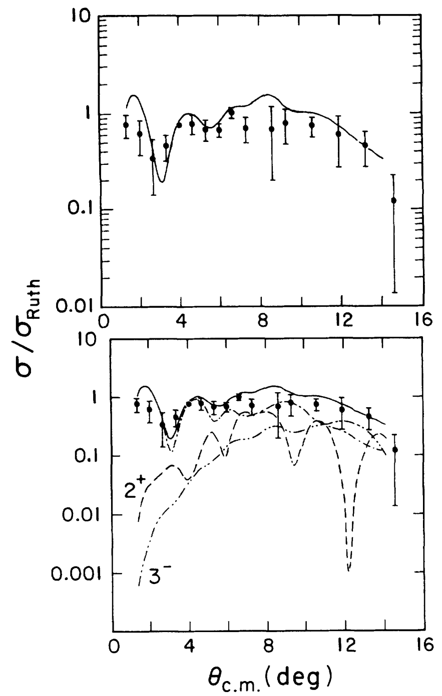

FIG. 4. The angular distribution for quasielastic scattering of ^{14}Be on ^{12}C at an incident energy of 796 MeV (upper). The solid curve is a calculation with the phenomenological ^{14}Be optical-model potential given in Table I. The lower panel illustrates the separate elastic and inelastic components of the distribution, as in Fig. 3.

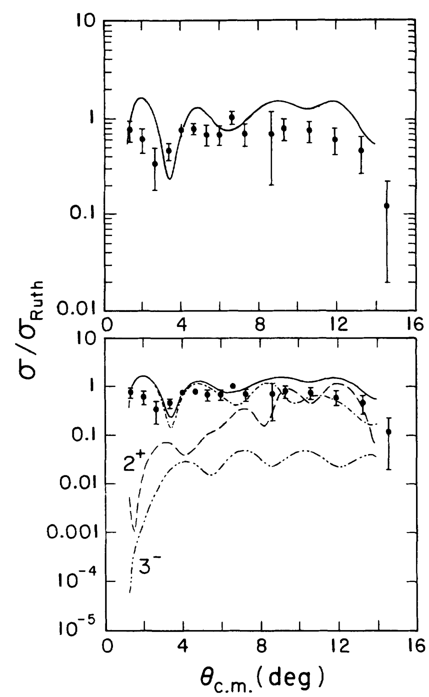

FIG. 5. As in Fig. 4, except that the optical-model potential is that for ^{12}Be in Table I, but with W = 77.97 MeV and W_s = 1.865 MeV. See text for further discussion.

neutron "halo." In addition, the observed structure is shifted to smaller angles; part of this shift is due to the fact that these angular distributions were measured at the same energy per nucleon rather than the same momentum. The solid curve in Fig. 4 (upper) is again the "best fit" result of a phenomenological optical-model analysis, and it has χ^2/N=2.1. The individual components of the curve given in the upper part of Fig. 4 are illustrated in the lower part of the figure. The parameters of the corresponding potential are given in Table I, and compared there with the potential for ^{11}Li scattering given in Ref. [7]. In view of the rather different behavior of the ^{11}Li [3] and ^{14}Be angular distributions at the nearside/farside interference minimum in the vicinity of 4° (which is almost completely absent in the ^{11}Li case), it is perhaps surprising that we were unable to fit the present data set without the use of an attractive surface real potential which is qualitatively similar to that used by Mermaz to fit our ^{11}Li angular distribution. A major difference between the surface-real parts of these two potentials, however, is the much smaller diffuseness in the present case, which also implies a weaker potential since the depth of a normalized Woods-Saxon derivative potential contains the diffuseness as one of its factors. The reduced diffuseness carries over to the imaginary surface term since a_{is} is also about a factor of 2 smaller here than in the corresponding ^{11}Li potential (see Table I).

As an illustration of the effects that lead to the introduction of a surface-real term, Fig. 5 shows the result of an attempt to fit the ^{14}Be angular distribution using the ^{12}Be parameters from Table I. Of course, this potential cannot be used directly because of the differences in the absorption referred to above; Fig. 5 gives the result of a fit in which the free parameters were the depths of the volume- and surface-imaginary potentials. This fit has χ^2/N=11. On the other hand, one might also take the best-fit ^{14}Be potential, eliminate the surface-real potential, and adjust the diffuseness of the volume-real potential to partially compensate for this change. The result of this procedure, shown in Fig. 6, has χ^2/N = 5.3, but is qualitatively in worse agreement with experiment than the fit given in Fig. 5. A careful comparison of these two figures shows that one major effect of the attractive surface-real potential is to shift the structure in the angular distribution to smaller angles, in better agreement with experiment. As mentioned above, part of the observed shift is due to the fact that the incident momenta are different in the two cases; however, it now appears that some of the shift results from the different structures of ^{14}Be and ^{12}Be, leading to a potential that is somewhat more refractive in the surface region in the former case.

The total reaction cross section calculated from the ^{14}Be potential in Table I is 1900 mb. Using Eqs. (1) and (2) above, the predicted value is 1648 mb (including the neutron-excess term). However, Tanihata *et al.* [13] have measured a radius of 3.11 fm for ^{14}Be, compared with the value of 2.65 fm which results from Eq. (1). The former value yields a predicted total reaction cross section of 1957 fm, in excellent agreement with experiment. The implication is that a neutron-excess term with coefficient α = 5 fm (as in Refs. [11] and [12]) is necessary to fit the total reaction cross section for ^{14}Be, while the ^{12}Be data

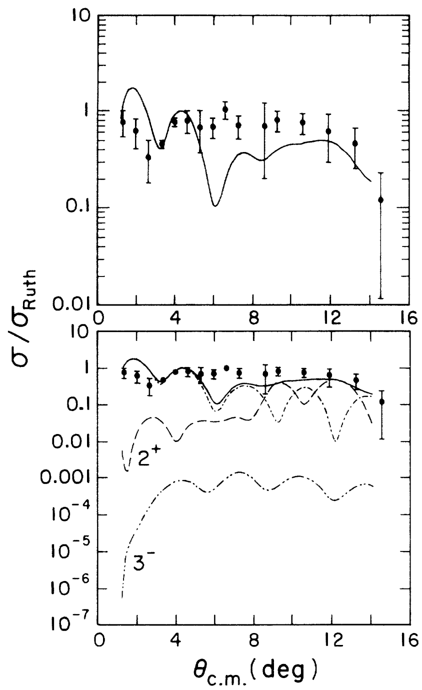

FIG. 6. As in Fig. 4, except that the optical-model potential is that for ^{14}Be in Table I, but with $V_s = 0.0$ MeV and $a_0 = 0.7357$ fm. See text for further discussion.

favor $\alpha = 1$ fm. Shen Wen-qing *et al.* [12] have associated the neutron-excess term with the surface diffusiveness of the nuclear potential. In that case, one might expect "neutron halo" nuclei to exhibit a larger isotope effect as seen here. This effect should disappear at energies above about 100 MeV per nucleon, where the differences between the *np* cross section and the *nn* and *pp* cross section start to become negligible.

In conclusion, we have measured the quasielastic-scattering cross sections for the interaction of ^{12,14}Be with ^{12}C, and compared them with phenomenological optical-model calculations in which inelastic scattering to the first 2^+ excited state in ^{12}C was treated in the coupled-channels approach. A good fit was obtained to the ^{12}Be+^{12}C angular distribution using a potential that has a deep volume-imaginary term and a very small surface-imaginary part. The corresponding total reaction cross section of 1238 mb is in accord with expectations from the systematics of heavy-ion reaction cross sections at intermediate energies. The ^{14}Be+^{12}C angular distribution, however, requires a potential with a much deeper surface-imaginary component, together with an attractive surface-real part, in order to obtain a reasonably good fit. This is qualitatively the same phenomenon as that observed by Mermaz in his analysis of the ^{11}Li+^{12}C quasielastic data. The total reaction cross section of 1900 mb is very large, though it can be accommodated within the systematics if one adopts a neutron-excess term of the same magnitude as that needed to account for the isotope effect in the Ni region, for example. It should be emphasized that, though the extracted total reaction cross section can be quite sensitive to the absolute normalization of the experimental data, the present ^{12,14}Be angular distributions were measured via the same method and in the same experiment. Further investigation of the neutron-excess term in the elastic scattering of exotic radioactive nuclear beams is clearly important; these studies are best carried out in the energy region from 30 to 60 MeV per nucleon where the differences in the various nucleon-nucleon cross sections are large. Finally, it will be interesting to compare the quasielastic-scattering angular distributions with Glauber-model calculations as in Ref. [6], to investigate the sensitivity to the assumed structure of the ^{14}Be ground state. Such calculations will soon become available [14].

Support for this work was provided by the U.S. National Science Foundation under Grant Nos. PHY91-00688 and PHY92-14992, and the U.S. Dept. of Energy under Contract No. W-31-109-ENG-38.

[1] A. C. Mueller and B. M. Sherrill, Annu. Rev. Nucl. Part. Sci., Vol. 43, 529 (1993).
[2] P. G. Hansen, Nucl. Phys. **A553**, 89c (1993).
[3] J. J. Kolata *et al.*, Phys. Rev. Lett. **69**, 2631 (1992).
[4] C. B. Moon *et al.*, Phys. Lett. B **297**, 39 (1992).
[5] M. Lewitowicz *et al.*, Nucl. Phys. **A562**, 301 (1993).
[6] I. J. Thompson, J. S. Al-Khalili, J. A. Tostevin, and J. M. Bang, Phys. Rev. C **47**, R1364 (1993).
[7] Michel C. Mermaz, Phys. Rev. C **47**, 2213 (1993).
[8] J. Raynal, in *Applied Nuclear Theory and Nuclear Model Calculations for Nuclear Technology Applications*, edited by M. K. Mehta and J. J. Schmidt (World Scientific, Singapore, 1988), p. 506.
[9] S. Raman, C. H. Malarkey, W. T. Milner, C. W. Nestor, Jr., and P. H. Stelson, At. Data Nucl. Data Tables **36**, 19 (1987).
[10] R. H. Spear, At. Data Nucl. Tables **42**, 81 (1989).
[11] S. Kox *et al.* Phys. Rev. C **35**, 1678 (1987).
[12] Shen Wen-qing *et al.*, Nucl. Phys. **A491**, 130 (1989).
[13] I. Tanihata *et al.*, Phys. Lett. B **206**, 592 (1988).
[14] I. J. Thompson, private communication.